ACS APPLIED MATERIALS & INTERFACES

Letter

www.acsami.org

Corrugated Sapphire Substrates for Organic Light-Emitting Diode Light Extraction

Wooram Youn, Jinhyung Lee, Minfei Xu, Rajiv Singh, and Franky So*

Department of Materials Science and Engineering, University of Florida, Gainesville, Florida 32611-6400, United States

Supporting Information

ABSTRACT: In an organic light-emitting diode (OLED), only about 20−30% of the generated light can be extracted because of the light lost to the thin film guided modes and surface plasmon. Using corrugated high-index-refractive substrates, the thin film guided modes can be effectively out-coupled from the device because of the high index substrate and the loss to the surface plamon is suppressed due to the corrugated structure. With an additional macro lens attached to the substrate to extract the substrate mode, we finally demonstrated a green phosphorescent OLED with an extremely high external quantum efficiency of 63%.

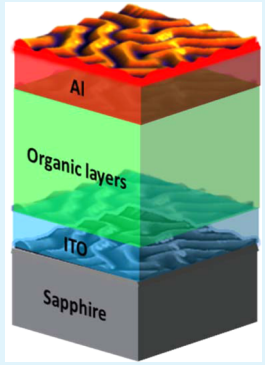

KEYWORDS: *OLED, surface plasmon mode, light extraction, high-refractive-index substrate*

Organic light-emitting diodes (OLEDs) have become a promising candidate for lighting applications due to their flexibility, low-power consumption and excellent color quality. However, the low extraction efficiency in OLEDs still remains as the biggest challenge for lighting applications. Although the internal quantum efficiency has reached close to 100% using phosphorescent emitters, the external quantum efficiency is typically about 25%.[1−3]

The low extraction efficiency in OLEDs is due to the difference in refractive indices between air (n = 1), the glass substrate ($n \approx 1.5$), and the organic/ITO (1.7−2) layers. In conventional OLEDs, only 20−30% of the generated light can escape into air and another 20−30% is trapped in the substrate,[4] and the rest of the emitted light is trapped and guided in the organic/ITO layers. Depending on where the optical modes are located in the ITO/organic layers, they can be categorized into waveguided modes that mostly concentrate closed to the ITO layer and surface plasmon (SP) mode that propagates as surface waves along the metal−organic interface, accounting for close to 50% of the total light output in an optimized OLED.[5]

To improve the light extraction efficiency, researchers have introduced various techniques. The substrate mode can be extracted effectively using microlens arrays and light scattering layers.[6−8] Waveguided modes can be extracted using photonic crystals, low-index grids, and high-index substrates.[9−15] Especially, using high-index substrates with a refractive index similar to that of the organic/ITO layers, the waveguided modes can be significantly suppressed. Leo et al.[15] reported white OLEDs fabricated on high-refractive-index substrates, resulting in a ∼50% enhancement in external quantum efficiency (EQE). To minimize the efficiency loss due to the SP mode, one can either get rid of the metal electrode or use corrugated structures. To minimize the presence of the SP mode, Kim el al. have fabricated transparent OLEDs without the metal electrode and achieved an EQE of 65%. To extract the SP mode, corrugated OLEDs have been shown to be very effective.[16−21] Specifically, corrugated OLEDs fabricated on buckling structures with a semirandom periodicity have shown to give significant enhancements in efficiency across the entire visible spectrum.[16] Although the techniques mentioned above are effective to extract either the thin-film guided modes or the SP modes, there has not been a demonstration of effective out-coupling of both thin-film and SP modes simultaneously.

Here, we report a scheme to extract the waveguided, SP and substrate modes simultaneously in an OLED. By fabricating OLEDs on corrugated high-refractive-index sapphire substrates (n ∼ 1.8), extraction of both the waveguided and SP modes was fully exploited. Using an additional macro lens on the back side of the substrate to extract the substrate mode, we were able to realize a green phosphorescent OLED with an EQE of 63% and a current efficiency of 225 cd/A. Unlike the conventional photonic crystals, which are effective only for light extraction at specific wavelengths, the quasi-periodic corrugated structure can enhance the extraction in all wavelengths with an emission profile similar to that of a Lambertian emitter.

The fabrication process for the corrugated sapphire substrates consists of three steps: (i) coating a monolayer of silica sphere arrays by Langmuir−Blodgett (LB) technique on

Received: February 16, 2015
Accepted: April 20, 2015
Published: April 20, 2015

DOI: 10.1021/acsami.5b01533
ACS Appl. Mater. Interfaces 2015, 7, 8974−8978

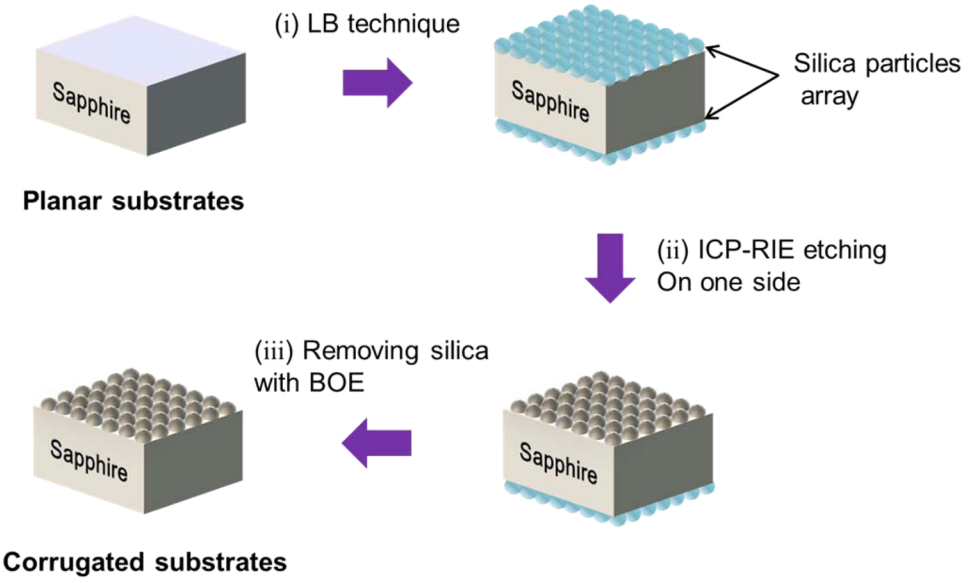

Figure 1. Schematic diagram of the fabrication process for the quasi-periodic hemisphere pattern sapphire substrate.

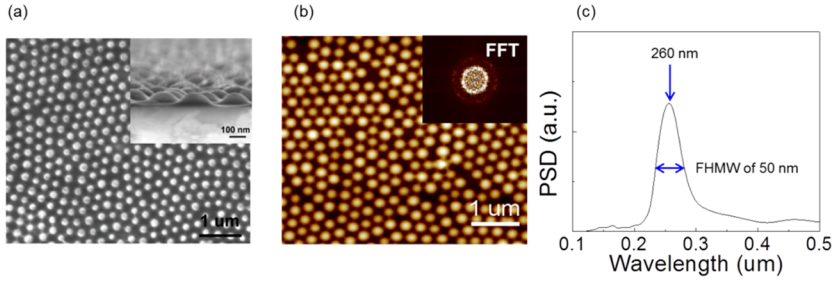

Figure 2. (a) Top-view of SEM image on corrugated sapphire substrate. Inset: cross-section view of the nanostructured sapphire substrate. (b) AFM image of the corrugated sapphire substrate fabricated with 275 nm silica spheres (Dimensions, 5 × 5 μm^2). Inset: fast Fourier transform (FFT) pattern of the corresponding image. (c) Power spectra from FFT as a function of periodicity for the pattern. Nominal periodicity of 260 nm with a full width at half-maximum (FHMW) of 50 nm, indicating a broad distribution of the periodicity.

sapphire substrates, (ii) transferring the pattern of silica sphere arrays to the top of the sapphire substrate by inductively coupled plasma reactive ion etching (ICP-RIE), and (iii) removing the silica spheres on the back side of the substrate with buffered oxide etch. The schematic diagrams of these processing steps are illustrated in Figure 1. To fabricate the sacrificial masks for patterning the sapphire substrate, monodispersed silica spheres with a diameter of 275 nm were self-assembled to form a quasi-periodic array on the substrates using a LB trough, and the details have been documented in previous work.[18] To fabricate the corrugated structure on the sapphire substrates, we used 10 sccm of BCl_3, 25 sccm of Cl_2, and 10 sccm of Ar in a plasma etcher at a radio frequency power of 450 W and a coil power of 125 W to etch both the silica spheres and the sapphire substrates at the same time. To maximize the depth of the corrugated structure, the substrate was exposed to the plasma until the silica spheres were completely removed. Using this process, hemispheres are formed on the sapphire substrate with a periodicity close to the diameters of the silica particles. The corrugated structure was characterized using scanning electron microscopy (SEM) and atomic force microscopy (AFM), and the results are shown in Figure 2a, b. The AFM and SEM images show the quasi-periodic pattern fabricated. The diffused ring pattern in the fast Fourier transform (FFT) patterns shown in the inset of Figure 2b confirms that the grating wave vectors are over all azimuthal directions, allowing outcoupling of the SP mode over all azimuthal angles. Figure 2c represents the power spectrum of the corrugated structure, which shows a nominal periodicity of 260 nm with a full width at half-maximum of 50 nm, indicating a broad range of grating wave vectors. The SEM image in the inset of Figure 2a shows the cross-sectional-view corrugated structure of the sapphire substrate with a depth of about 80−90 nm, which can effectively diffract the SP modes. For direct comparison, green phosphorescent OLEDs were fabricated on both corrugated and planar high-refractive-index substrates and the details of device structure can be found in the Supporting Information.

To analyze the optical modes in OLEDs fabricated on sapphire substrates, we calculated the dispersion curve using transfer matrix method and the results are shown in Figure 3a. Here, the refractive indices of ITO and Al were taken from our previous work and published literatures.[13,21−23] For simplicity, the effect of the LiF layer was ignored because of the extremely thin layer used (1 nm) compared with other layers and the thicknesses of the substrate and the Al layer were considered semi-infinite.[24] The calculated dispersion curve shows that only the SP mode can be excited inside of OLEDs on high-refractive-index substrates. It should be noted that for the devices fabricated on sapphire substrates, the waveguided modes are not present because they are coupled into the

DOI: 10.1021/acsami.5b01533
ACS Appl. Mater. Interfaces 2015, 7, 8974−8978

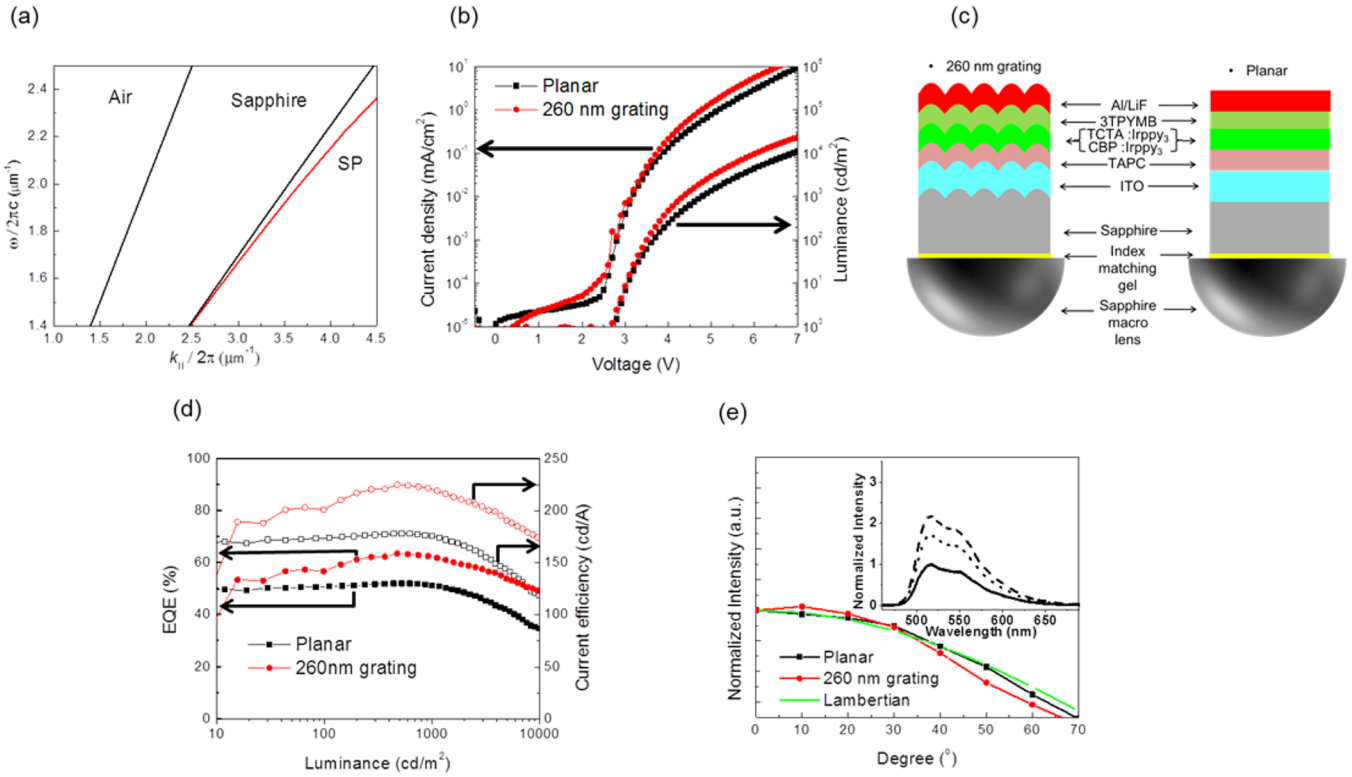

Figure 3. (a) Dispersion curves calculated by transfer matrix method. The solid lines represent the light lines for air and sapphire substrate modes. (b) *L*−*V*−*J* curves for both plain (black) and corrugated (red) OLEDs. (c) Corrugated 260 nm grating and planar device structures. (d) Current efficiency (cd/A) and external quantum efficiency (%) for the 260 nm periodicity grating (red) and reference (black) devices (e) Angular measurements in normal direction for both OLEDs with planar (black) and corrugated structures (red). For comparison, the ideal Lambertian pattern (green) is plotted as well. Inset: Substrate mode extraction of devices fabricated on both planar glass (dot) and sapphire (dash) substrates by a macro lens.

sapphire substrate, and hence more light is expected to be trapped inside the substrate.

With the presence of an in-plane component of the grating wave vector in the corrugated OLEDs, the SP modes can be effectively extracted. Specifically, for emitters such as $Ir(ppy)_3$ with an emission wavelength maximum at 515 nm, the optimum periodicity of the grating for normal direction diffraction on the SP modes was determined to be in the range of 260−270 nm by transfer matrix method.[16,17] Here, we chose silica spheres with a periodicity of 275 nm to fabricate the corrugated structure on the sapphire substrates, and the resulting corrugated structure has a nominal periodicity of 260 nm.

Figure 3b shows the Luminance−Voltage−Current density (*L*−*V*−*J*) characteristics of OLEDs fabricated on corrugated and planar sapphire substrates with a macro lens. And the schematic device structures for both devices are shown in Figure 3(c). It is generally believed that the corrugated surface might lead to shorting in the devices. However, our data show that even with a corrugation depth of about 80−90 nm, it has no effect on the device leakage current and hence shorting is not a problem in our corrugated devices. On the other hand, the corrugation does increase carrier injection resulting in a higher current density in the corrugated OLEDs. While a part of current density enhancement is from the larger surface area of the corrugated structure than that of planar structure, the major enhancement in current density is attributed to the thickness variation and the enhanced electric field in the organic layers due to the corrugated structures.[16,18,25] In addition to the increase of current density, Figure 3b shows the enhanced luminance in the corrugated device due to extraction of the SP mode. Figure 3d shows both the current efficiency and EQE for both devices. The corrugated OLED shows a high current efficiency value of 225 cd/A and a high peak EQE value of 63%, whereas the planar device shows 178 cd/A and 52% in peak current efficiency and EQE, respectively. Compared to the OLED fabricated on planar sapphire substrates, the enhancement is ∼25% in both current efficiency and EQE. Because both devices were fabricated on sapphire substrates, waveguided modes are not present and the enhancement in the corrugated device must be coming from extraction of the SP mode. To confirm the enhanced substrate mode, planar OLEDs were fabricated on both conventional glass and sapphire substrates. When a macro lens was used for the devices, as shown in the inset of Figure 3e, 120% enhancement in light output was observed from the sapphire substrate, whereas only 70% enhancement from the glass substrate was observed, confirming that the enhanced substrate mode in the sapphire substrate is attributed to the transfer of the waveguided mode into the substrate mode in devices fabricated on sapphire substrates. As shown in Figure 3e, the corrugated OLED shows a Lambertian-like emission profile, indicating that the outcoupled SP mode is not angular-dependent because of the randomly distributed grating wave vectors with a broad magnitude. Because the nominal periodicity of 260 nm here diffracts the SP mode into the normal direction, a stronger intensity at normal direction than higher angles (40−60°) is observed in the corrugated device.

DOI: 10.1021/acsami.5b01533
ACS Appl. Mater. Interfaces 2015, 7, 8974−8978

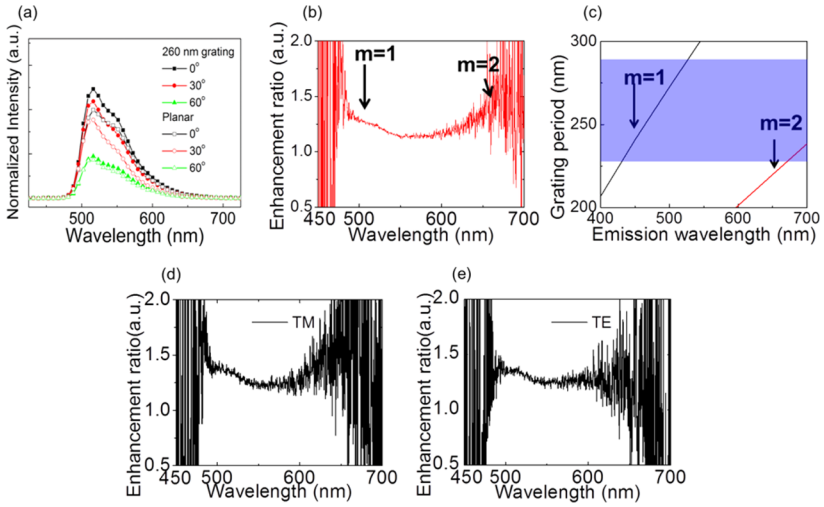

Figure 4. (a) Electroluminescence (EL) spectra for both OLEDs with planar (black) and corrugated structures (red) measured in three different angles. (b) EL intensity enhancement ratio between planar and corrugated OLEDs, plotted by dividing the EL spectrum of the grating device measure in normal direction by that of the planar device. Stronger enhancements at ~500 nm and ~650 nm are due to first-order (m = 1) and second-order (m = 2) diffraction, respectively. (c) Grating periodicity for normal direction diffraction on the SP mode as a function of emission wavelength. First- (black) and second-order (red) diffraction condition are satisfied by distributed periodicity of 260 nm grating structure (blue rectangular box). (d, e) Enhancement ratio of EL intensity of TM- and TE-polarization.

To further understand the origin of the light outcoupling due to the corrugated device, electroluminescence (EL) spectra for 0, 30, and 60° were measured on both corrugated and planar devices, and the results are shown in Figure 4a. It should be noted that all EL intensities of the corrugated devices are enhanced over all emission wavelengths for all three angles, further confirming the broad distribution of the grating wave vectors in the corrugated structure. To verify that the enhanced outcoupling is due to Bragg diffraction of the SP modes into the normal direction, the enhancement factor of the corrugated OLED, which is the ratio of the EL intensity of the corrugated OLED to that of the planar OLED was measured, and the results are shown in Figure 4b. This figure shows more pronounced enhancements at ~500 and ~650 nm. To understand the origin of the light outcoupling enhancements, we calculated the in-plane propagation vectors of the SP modes by transfer matrix method and plotted the grating periodicity as a function of the emission wavelength of the outcoupled light as shown in Figure 4c. Considering a nominal periodicity of 260 nm in the corrugated structure, the first order (m = 1) diffraction for the SP mode is responsible for the enhancement at wavelengths of ~500 nm. Similarly, the second order diffraction for the SP mode is responsible for the enhancement at wavelengths of ~650 nm as indicated in the blue region in Figure 4c. Thus, the strong enhancement in outcoupling at these two wavelengths from the corrugated OLED is a direct evidence of SP mode extraction via the first- and second-order diffractions. Additionally, we performed polarized EL measurements to determine the enhancement factor of the transverse magnetic(TM)- and transverse electric(TE)-polarized modes of the EL emission, and the results are shown in in Figure 4d, e. Generally, the excitation of the SP mode comes from the incident TM-polarized light on the metal−organic interface. As expected, the enhancement factor regarding TM polarization of the corrugated OLED from Figure 4d show a similar wavelength dependence compared to the data measured without the polarizer as shown in Figure 4b, satisfying the first- and second-order diffraction conditions. However, similar enhancements were also observed from the TE-polarized EL as shown in Figure 4e. Becausee the waveguided mode (TE mode) is not expected to be present in devices fabricated on sapphire substrates, the enhancements of the TE polarized light is due to polarization conversion resulting from diffraction in a quasi-periodic structure. This so-called conical diffraction,[26,27] from quasi-periodic structure has been previously reported in corrugated OLEDs.[17] Due to the randomly oriented grating wave vectors in all azimuthal angles, diffraction can convert the polarization from TM-polarized light to TE-polarized light, further confirming the extraction of the SP mode.

In summary, outcoupling of waveguided and SP modes were demonstrated with OLEDs fabricated on high-refractive-index corrugated substrates. With a macro lens to extract the substrate and thin film guide modes, the resulting OLEDs have a very high external quantum efficiency of 63% and a current efficiency of 225 cd/A. With this device architecture, the light extraction enhancement is independent of wavelength and the emission profile is similar to a Lambertian emitter, demonstrating that this device is promising for OLED lighting applications.

EXPERIMENTAL SECTION

For device fabrication, a sputtering system and a thermal evaporator were used for depositing the ITO electrodes and organic layers on both corrugated and planar sapphire substrates. The OLED has the following structure: a 120 nm thick ITO, a 45 nm thick TAPC (4,4′-Cyclohexylidenebis(N,N-bis(4-methylphenyl)benzenamine)), a 15 nm thick CBP (4,4′-Bis(N-carbazolyl)-1,1′-biphenyl) doped with Ir(ppy)3 (fac-tris(2-phenylpyridyl)Ir(III)), and 15 nm thick TCTA (tris(4-carbazoyl-9-ylphenyl)amine) doped with Ir(ppy)3, a 60 nm-thick 3TPYMB (tris(2,4,6-trimethyl-3-(pyridin-3-yl)phenyl)borane, a 1 nm thick lithium fluoride (LiF), and a 100 nm-thick aluminum (Al). The area of the devices is 2 mm × 2 mm. The devices were encapsulated with cover glass and UV-curable sealant in a nitrogen-ambient glovebox. A sapphire hemisphere lens with a diameter of 4 mm was attached to the backside of the sapphire substrate for extracting the substrate mode using index-matching gel with a refractive index of 1.76. For the devices fabricated on conventional glass substrates, a

DOI: 10.1021/acsami.5b01533
ACS Appl. Mater. Interfaces 2015, 7, 8974−8978

glass macrolens was attached to the substrate using an index matching gel with a refractive index of ~1.5.

For device characterization, a 10 in. diameter integrating sphere (Labsphere) with photodiode was used for collecting all photons emitted from the devices driven by a source meter (Keithley 2400). Electroluminescence (EL) spectra with and without a linear polarizer were recorded with same source meter and a spectrometer (Ocean Optics HR4000). The emission profile of the OLEDs was done by mounting the devices on a rotating stage.

■ ASSOCIATED CONTENT

Supporting Information

Details on device characterization (PDF). This material is available free of charge via the Internet at http://pubs.acs.org/.

■ AUTHOR INFORMATION

Corresponding Author

*E-mail: fso@mse.ufl.edu.

Notes

The authors declare no competing financial interest.

■ ACKNOWLEDGMENTS

The authors acknowledge the support of Department of Energy Solid State Lighting Program (Contract DE-FG0207ER46464).

■ REFERENCES

(1) Adachi, C.; Baldo, M. A.; Forrest, S. R.; Lamansky, S.; Thompson, M. E.; Kwong, R. C. High-Efficiency Red Electrophosphorescence Devices. *Appl. Phys. Lett.* **2001**, *78*, 1622−1624.

(2) Eom, S. H.; Zheng, Y.; Chopra, N.; Lee, J.; So, F.; Xue, J. Low Voltage and Very High Efficiency Deep-Blue Phosphorescent Organic Light-Emitting Devices. *Appl. Phys. Lett.* **2008**, *93*, 133309−133309.

(3) Polikarpov, E.; Swensen, J. S.; Chopra, N.; So, F.; Padmaperuma, A. B. An Ambipolar Phosphine Oxide-Based Host for High Power Efficiency Blue Phosphorescent Organic Light Emitting Devices. *Appl. Phys. Lett.* **2009**, *94*, 223304.

(4) Chutinan, A.; Ishihara, K.; Asano, T.; Fujita, M.; Noda, S. Theoretical Analysis on Light-Extraction Efficiency of Organic Light-Emitting Diodes Using FDTD and Mode-Expansion Methods. *Org. Electron.* **2005**, *6*, 3−9.

(5) Smith, L. H.; Wasey, J. A. E.; Samuel, I. D. W.; Barnes, W. L. Light Out-Coupling Efficiencies of Organic Light-Emitting Diode Structures and the Effect Of Photoluminescence Quantum Yield. *Adv. Funct. Mater.* **2005**, *15*, 1839−1844.

(6) Eom, S. H.; Wrzesniewski, E.; Xue, J. Close-Packed Hemispherical Microlens Arrays for Light Extraction Enhancement in Organic Light-Emitting Devices. *Org. Electron.* **2011**, *12*, 472−476.

(7) Cheng, Y. H.; Wu, J. L.; Cheng, C. H.; Syao, K. C.; Lee, M. C. M. Enhanced Light Outcoupling in a Thin Film by Texturing Meshed Surfaces. *Appl. Phys. Lett.* **2007**, *90*, 091102.

(8) Chen, S. M.; Kwok, H. S. Light Extraction from Organic Light-Emitting Diodes for Lighting Applications by Sand-Blasting Substrates. *Opt. Express* **2010**, *18*, 37−42.

(9) Lee, Y. J.; Kim, S. H.; Huh, J.; Kim, G. H.; Lee, Y. H.; Cho, S. H.; Kim, Y. C.; Do, Y. R. A High-Extraction-Efficiency Nanopatterned Organic Light-Emitting Diode. *Appl. Phys. Lett.* **2003**, *82*, 3779−3781.

(10) Ishihara, K.; Fujita, M.; Matsubara, I.; Asano, T.; Noda, S.; Ohata, H.; Hirasawa, A.; Nakada, H.; Shimoji, N. Organic Light-Emitting Diodes with Photonic Crystals on Glass Substrate Fabricated by Nanoimprint Lithography. *Appl. Phys. Lett.* **2007**, *90*, 111114.

(11) Sun, Y.; Forrest, S. R. Enhanced Light Out-Coupling of Organic Light-Emitting Devices Using Embedded Low-Index Grids. *Nat. Photonics* **2008**, *2*, 483−487.

(12) Mladenovski, S.; Neyts, K.; Pavicic, D.; Werner, A.; Rothe, C. Exceptionally Efficient Organic Light Emitting Devices Using High Refractive Index Substrates. *Opt. Express* **2009**, *17*, 7562−7570.

(13) Gu, G.; Garbuzov, D. Z.; Burrows, P. E.; Venkatesh, S.; Forrest, S. R.; Thompson, M. E. High-External-Quantum-Efficiency Organic Light-Emitting Devices. *Opt. Lett.* **1997**, *22*, 396−398.

(14) Meerheim, R.; Furno, M.; Hofmann, S.; Lussem, B.; Leo, K. Quantification of Energy Loss Mechanisms in Organic Light-Emitting Diodes. *Appl. Phys. Lett.* **2010**, *97*, 253305.

(15) Reineke, S.; Lindner, F.; Schwartz, G.; Seidler, N.; Walzer, K.; Lussem, B.; Leo, K. White Organic Light-Emitting Diodes with Fluorescent Tube Efficiency. *Nature* **2009**, *459*, 234−238.

(16) Koo, W. H.; Jeong, S. M.; Araoka, F.; Ishikawa, K.; Nishimura, S.; Toyooka, T.; Takezoe, H. Light Extraction from Organic Light-Emitting Diodes Enhanced by Spontaneously Formed Buckles. *Nat. Photonics* **2010**, *4*, 222−226.

(17) Koo, W. H.; Jeong, S. M.; Nishimura, S.; Araoka, F.; Ishikawa, K.; Toyooka, T.; Takezoe, H. Polarization Conversion in Surface-Plasmon-Coupled Emission drom Organic Light-Emitting Diodes Using Spontaneously Formed Buckles. *Adv. Mater.* **2011**, *23*, 1003−1007.

(18) Koo, W. H.; Youn, W.; Zhu, P. F.; Li, X. H.; Tansu, N.; So, F. Light Extraction of Organic Light Emitting Diodes by Defective Hexagonal-Close-Packed Array. *Adv. Funct. Mater.* **2012**, *22*, 3454−3459.

(19) Frischeisen, J.; Yokoyama, D.; Adachi, C.; Brutting, W. Determination of Molecular Dipole Orientation in Doped Fluorescent Organic Thin Films by Photoluminescence Measurements. *Appl. Phys. Lett.* **2010**, *96*, 073302.

(20) Kim, S. Y.; Jeong, W. I.; Mayr, C.; Park, Y. S.; Kim, K. H.; Lee, J. H.; Moon, C. K.; Brutting, W.; Kim, J. J. Organic Light-Emitting Diodes with 30% External Quantum Efficiency Based on a Horizontally Oriented Emitter. *Adv. Funct. Mater.* **2013**, *23*, 3896−3900.

(21) Kim, J. B.; Lee, J. H.; Moon, C. K.; Kim, S. Y.; Kim, J. J. Highly Enhanced Light Extraction from Surface Plasmonic Loss Minimized Organic Light-Emitting Diodes. *Adv. Mater.* **2013**, *25*, 3571−3577.

(22) Wang, Z. B.; Helander, M. G.; Qiu, J.; Puzzo, D. P.; Greiner, M. T.; Hudson, Z. M.; Wang, S.; Liu, Z. W.; Lu, Z. H. Unlocking the Full Potential of Organic Light-Emitting Diodes on Flexible Plastic. *Nat. Photonics* **2011**, *5*, 753−757.

(23) Yokoyama, D.; Nakayama, K.; Otani, T.; Kido, J. Wide-Range Refractive Index Control of Organic Semiconductor Films Toward Advanced Optical Design of Organic Optoelectronic Devices. *Adv. Mater.* **2012**, *24*, 6368−6373.

(24) Fuhrmann, T.; Samse, K.; Salbeck, J.; Perschke, A.; Franke, H. Guided Electromagnetic Waves in Organic Light Emitting Diode Structures. *Org. Electron.* **2003**, *4*, 219−226.

(25) Fujita, M.; Ueno, T.; Ishihara, K.; Asano, T.; Noda, S.; Ohata, H.; Tsuji, T.; Nakada, H.; Shimoji, N. Reduction of Operating Voltage in Organic Light-Emitting Diode by Corrugated Photonic Crystal Structure. *Appl. Phys. Lett.* **2004**, *85*, 5769−5771.

(26) Inagaki, T.; Goudonnet, J. P.; Little, J. W.; Arakawa, E. T. Photoacoustic Study of Plasmon-Resonance Absorption in a Bigrating. *J. Opt. Soc. Am. B* **1985**, *2*, 433−439.

(27) Inagaki, T.; Goudonnet, J. P.; Arakawa, E. T. Plasma Resonance-Absorption in Conical Diffraction - Effects of Groove Depth. *J. Opt. Soc. Am. B* **1986**, *3*, 992−995.

DOI: 10.1021/acsami.5b01533
ACS Appl. Mater. Interfaces 2015, 7, 8974−8978